Journal of
Applied Crystallography

ISSN 0021-8898

Received 20 October 2009
Accepted 4 March 2010

Scatter: software for the analysis of nano- and mesoscale small-angle scattering

S. Förster,[a]* L. Apostol[b] and W. Bras[b]

[a]Institut für Physikalische Chemie, Universität Hamburg, Grindelallee 117, 20146 Hamburg, Germany, and [b]DUBBLE, ESRF, Avenue des Martyrs, 38043 Grenoble, France. Correspondence e-mail: forster@chemie.uni-hamburg.de

Scatter is a new software for analysis, modeling and fitting of one- and two-dimensional small-angle scattering data of non-ordered, partially ordered or fully ordered nano- and mesoscale structures. The calculations are based on closed analytical expressions for the scattering intensity, enabling efficient evaluation of form factors and structure factors. The software allows one to sequentially fit large series of scattering curves and scattering patterns automatically. It provides further tools for data loading, beam centering, calibration, zooming, binning, lattice identification, calculation of density profiles and size distributions, and visualization of real-space structures. Presentations of experimental and calculated data can be saved as is for presentations or exported for further graphical or mathematical treatment.

1. Introduction

Modern materials science is achieving amazing control in assembling materials to provide desired functions and properties. Nanoscale building blocks of high regularity in size, shape and crystallinity are assembled into well defined ordered superstructures. The structures that can be realized become increasingly complex, consisting of multiple components and materials with sometimes hierarchically structured levels. For the characterization of structural properties such as geometry, regularity, periodicity, order and orientation, scattering and diffraction techniques are naturally the most adequate methods. They are intrinsically sensitive to periodic and regular features since they detect the Fourier transform of the structure.

Small-angle scattering (SAS) techniques using X-rays and neutrons are widely used for nano- and mesoscale characterization of materials. The latest generation synchrotron and neutron sources provide X-ray and neutron beams with vastly improved brilliance. At synchrotrons, submicrometre spot sizes have been developed that enable high-resolution scanning of samples. Recent advances in detector technology have made large-area detectors available with significantly increased area density and faster read-out times. This allows one to follow structural changes *in-situ*, for example, during processing or changes of external parameters. Knowledge, understanding and control of these changes becomes increasingly important in materials science.

The developments in source brilliance and detector performance have led to data productivity rates that are orders of magnitude higher than before, generating terabytes of data in minutes, which then await analysis. It becomes more and more evident that the data analysis step is evolving into the bottleneck of the productivity of light sources. Already today large amounts of data accumulated at beamlines at substantial cost remain unevaluated because of the absence of adequate analysis tools.

Routines for SAS data processing can be subdivided into two steps – data reduction and data analysis. Reduction of SAS data is often closely related to the instrument design and setup, and a number of instrument-specific data reduction packages have been developed. A few data packages, such as *FIT2D* (Hammersley, 1997, 2009), *Nika* (Ilavsky, 2009) and *Datasqueeze* (Heiney, 2005, 2009), provide generic tools. They are capable of performing primary data analysis for a wide variety of data formats. *FIT2D* has been well established and is widely employed in the user community. Therefore it can serve as an intermediate platform for new SAS data analysis routines such as the one described in the following.

A small number of software packages for the analysis of SAS data from nano- and mesoscale materials are currently available. They analyze measured scattering curves either independently of any model – employing efficient inverse Fourier transform/deconvolution routines – or using calculated scattering curves of model structures that are fitted to the data (Pedersen, 1997). Well established software packages include *GIFT* (Bergmann *et al.*, 2000), *BioXTAS RAW* (Nielsen *et al.*, 2009), *SASFit* from the Paul Scherrer Institute (Kohlbrecher, 2009), *FISH* from ISIS (Heenan, 2009), and tools based on the *Igor Pro* commercial scientific analysis application (Wavemetrics, 2008) such as the NIST analysis tools (Kline, 2006) and Advanced Photon Source tool *Irena* (Ilavsky, 2009; Ilavsky & Jemian, 2009).

For the analysis of two-dimensional scattering patterns there are fewer routines available. If the two-dimensional data can be reduced to one-dimensional data the analysis becomes much simpler and software packages are available. This is the case for diffraction patterns of single crystals that can be reduced to the integrated intensity of discrete sets of peaks. For isotropic samples or powder diffraction patterns, the two-dimensional data can be reduced to one-dimensional data by azimuthal averaging. Scattering patterns of materials with less regularity cannot be easily processed using such data reduction methods. Often the scattering patterns have to be treated as a whole. The number of data points and the demands on the software handling it are much more challenging. For the special case of samples with fiber symmetry (Squire *et al.*, 2003) and grazing incidence small-angle scattering (GISAS) (Lazzari, 2009), routines

are available. For the more general case of oriented, partially ordered or fully ordered structures, no software for modeling and fitting of scattering patterns currently exists.

For the analysis of large series of one- and two-dimensional scattering data, automated data analysis would greatly reduce the effort required to identify the proper analysis procedure and put the structural parameters in the framework of a suitable model. In particular, if the experimental configuration (wavelength, sample–detector distance, beam position) is fixed, which is often the case for *in-situ* time-resolved experiments, modeling and fitting could be performed sequentially for a large series of files without requiring user attention (Konarev *et al.*, 2006). To minimize the risk of improper analysis, the significance of the obtained fit needs to be evaluated for each data set. Warnings should be given in the case that unreliable or unphysical structural parameters are obtained.

In view of the need for software that is capable of analyzing one- and two-dimensional SAS data with the possibility of automated analysis we developed the program *Scatter* with the aim of fulfilling the following requirements:

(*a*) Analysis/modeling/fitting of one- and two-dimensional SAS and GISAS data.

(*b*) Automated and monitored analysis of large series of one- and two-dimensional data files.

(*c*) Use of advanced scattering/diffraction theory and mathematics.

(*d*) Fast file loading and calculation routines.

(*e*) Visualization of real-space structures.

(*f*) License-free, open source, running on Windows and freely distributable.

In the following we describe the main features of *Scatter* with examples taken from synchrotron SAXS experiments at DESY and ESRF. *Scatter* is available as an executable file running on Windows. The software can be downloaded free of charge at http://www.chemie.uni-hamburg.de/pc/sfoerster/software.html. It is accompanied by a manual that makes the user familiar with the various functions and tools of the software. Data in the form of scattering curves and scattering patterns exported from *FIT2D* (*.chi, *.spr) can be imported, providing access to a large number of data formats. The software has been written in Pascal/Delphi. It has already been used by many research groups worldwide for the analysis of SAS data.

2. One-dimensional data analysis, modeling and fitting

For the analysis of one-dimensional scattering data, *Scatter* provides tools for reading a variety of data formats, background subtraction, and a choice of a large number of form factors and structure factors. Parameters that are used for modeling or results from fitting can be stored in a parameter file for documentation. These parameter files can later be loaded to continue with the analysis. The graphical user interface (GUI) provides all relevant information for viewing, modeling and fitting of the data. Additional information and parameters are accessible in separate windows.

2.1. Data input and GUI

Input data formats are columnar ASCII spreadsheets where the scattering vector q is contained in the first column, the scattered intensity $I(q)$ in the second column and the statistical error of the intensity $\Delta I(q)$ (one standard deviation) in the third column. Standard formats are *EXCEL* type (*.csv), *GIFT* type (*.pri; O. Glatter), *FIT2D* type (*.chi; A. Hammersley) or *ESRF/ID02* type (*.out). The primary output data format is a columnar ASCII spreadsheet in *EXCEL* comma-delimited data format (*.csv), which can be imported in standard graphics software packages. It is possible to generate errors (percent errors or square-root errors) when errors are not provided in the data file. Data modifications other than binning are not foreseen in the software.

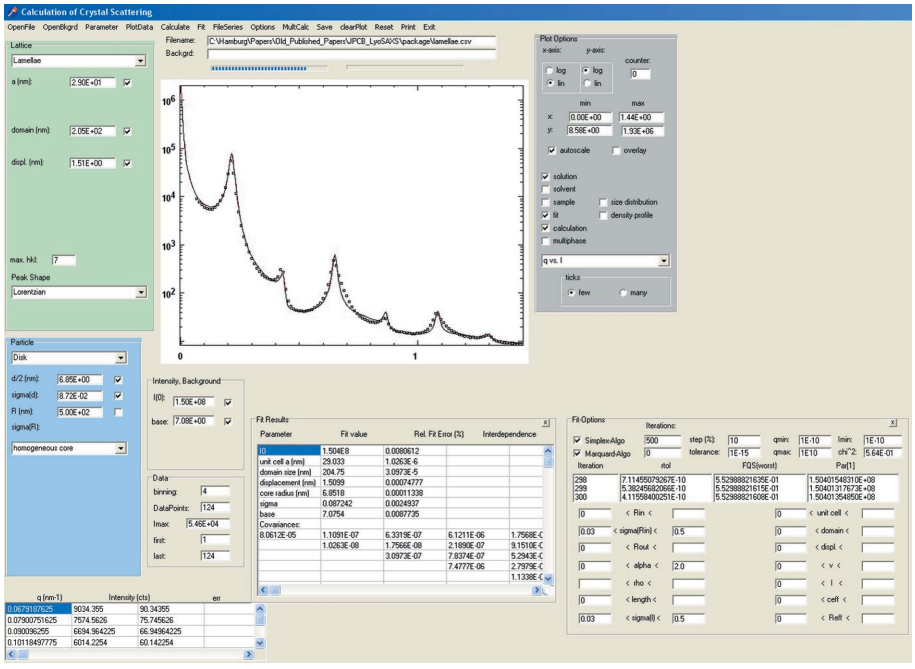

Figure 1
Typical example of the GUI for one-dimensional analysis, providing information on the particle lattice (green input field), particle structure (blue input field), plot options (gray field) and data. Detailed information on fit parameters, standard deviations, covariances and fitting algorithms are given in the corresponding tables. The measured scattering curve is from a lyotropic lamellar liquid crystal measured with synchrotron SAXS at HASYLAB/DESY.

The GUI for the one-dimensional analysis is shown in Fig. 1. It provides all relevant information for viewing, modeling and fitting of experimental data. It allows reading of experimental and background data, binning, and loading and saving of parameter files, and provides various plotting options (lin/log, autoscale, overlay, Guinier, Zimm, Holtzer, Krakty, Porod) for the scattered intensity. Linearized presentations of the scattering intensity are automatically analyzed to give the radius of gyration (Guinier plot) or the intercept and slope from which the radius of gyration (Zimm), molecular weight (Zimm), mass per unit length (Holtzer) or specific surface area (Porod) can be calculated. The GUI also guides model calculations and data fitting. It is possible to save experimental data, model calculations, fitted curves, size distributions and density profiles as ASCII data. The graphical data display can be saved as a bitmap and the whole GUI can be printed as a hard copy.

The GUI is organized into different boxes and tables. Information about the particle structure is contained in a green box, that

about the structure factor in a blue box and plotting options in a gray box (see Fig. 1). Different tables display experimental data, data information, fitting constraints and fit results. Additional information, such as a list of peak positions, as well as Porod and displacement analysis, can optionally be displayed.

Scatter provides various tools for identification of crystalline lattices. It can display peak positions superimposed on the experimental data with the first reflection at the position of the cursor in the window. Another option indexes each peak at the cursor position and gives the exact q value [$q = (4\pi\sin\theta)/\lambda$, θ being half the scattering angle and λ the wavelength]. It is also possible to perform multiphase calculations, where scattering curves for up to three different structures can be stored and their weighted sums calculated, displayed and superimposed with the data.

2.2. Form factors

Form factors for the most common geometrical and polymeric structures, such as spheres, cylinders, discs, uni- and multilamellar vesicles, Kratky–Porod chains, and excluded volume chains, are provided. The calculations take into account size distributions of cross-sectional radii (spheres, cylinders) and thicknesses (discs). Form factors for anisometric shapes (cylinders, discs) are averages over an isotropic orientational distribution. For vesicles, distributions over the bilayer thickness and the vesicle radii are taken into account. For all size distributions, a Schulz–Zimm distribution is used.

For geometrical objects (spheres, cylinders, discs, vesicles) the form factors $P(q)$ are calculated from the scattering amplitudes $F(q)$, which are expressed in terms of hypergeometric functions, *i.e.* (Förster & Burger, 1998)

$$\langle P(q)\rangle = \langle F^2(q)\rangle = \left\langle {}_0F_1^2\left(\frac{d+2}{2}; -\frac{q^2R^2}{4}\right)\right\rangle, \tag{1}$$

where the dimensionality is $d = 3$ for spheres, $d = 2$ for cylinders and $d = 1$ for discs. The angular brackets $\langle\cdots\rangle$ refer to an average over size and orientational distribution functions. R is the cross-sectional radius of a sphere or a cylinder, or half the thickness of a disc or vesicle bilayer. Because of their recursive definition, hypergeometric functions can be efficiently evaluated to arbitrary precision. Special functions such as Hermite, Bessel, Laguerre and Legendre functions can be expressed as hypergeometric functions and thus can be efficiently evaluated. Since the averages over Schulz–Zimm-type distributions lead again to hypergeometric functions, all form factors are obtained in closed analytical form so that calculations and fitting procedures are fast. The excluded volume chain calculation and the calculation of the sine integral for thin cylinders are also based on hypergeometric functions. For the Kratky–Porod chain, an analytical form of the pair correlation function given by Koyama (1973) is used.

It is straightforward to extend equation (1) to geometrical objects that have a core/shell structure consisting of a homogeneous core and a homogeneous or inhomogeneous shell (Förster & Burger, 1998). Inhomogeneous shells are assumed to have an algebraic density profile of the form $\rho(r)\tilde{r}^{\alpha}$, *i.e.* a scaling law that is typically expected for polymeric shells exhibiting a spherical, cylindrical or planar brush-like structure.

2.3. Structure factors

The structure factor describes the spatial distribution of the geometrical or polymeric objects. Structure factors are available for liquid-like or ordered periodic arrays of geometrical and polymeric objects including lamellae, cylinders packed in hexagonal (*P*6/*mm*), square (*P*4/*mm*) or centered rectangular arrays (*cmm*), spheres arranged on simple cubic (*Pm*3*m*), body-centered cubic (b.c.c., *Im*3*m*), face-centered cubic (f.c.c., *Fm*3*m*), hexagonal close-packed (h.c.p, *P*6/*mmc*), body-centered tetragonal (*I*4/*mm*) or randomly stacked close-packed arrays, and ordered bicontinuous cubic structures, *i.e.* gyroid (G-surface, *Ia*3*d*), double diamond (D-surface, *Pn*3*m*) and the plumbers nightmare (*Im*3*m*). For liquid-like structures the Percus–Yevick (PY) structure factor is used.

The scattering intensity for ordered one-, two- and three-dimensional structures is calculated within the decoupling approximation (Kotlarchyk, 1983; Förster, Timmann *et al.*, 2005) where the scattered intensity $I(q)$ is given by

$$\begin{aligned} I(q) &= (b_1 - b_2)^2 \rho_{\rm N} P(q) S(q), \\ S(q) &= 1 + \beta(q)[Z(q) - 1] G(q). \end{aligned} \tag{2}$$

b_1 and b_2 are the scattering length densities of the particles and the surrounding matrix, $\rho_{\rm N}$ is the number density of the particles, $P(q)$ is the form factor of the objects, $S(q)$ is the structure factor, $\beta(q) = \langle F(q)\rangle^2/\langle F^2(q)\rangle$ the ratio of the squared scattering amplitude of the objects, $G(q)$ the Debye–Waller factor, and $Z(q)$ the lattice factor given by

$$Z(q) = \frac{(2\pi)^{d-1}}{n v_d} \sum_{\{hkl\}} \frac{m_{hkl} f_{hkl}^2}{q_{hkl}^{d-1}} L_{hkl}(q), \tag{3}$$

where n is the number of particles per unit cell, v_d is the volume ($d = 3$), area ($d = 2$) or long period ($d = 1$) of the d-dimensional unit cell, f_{hkl} is the unit-cell structure factor, m_{hkl} is the peak multiplicity, and $L_{hkl}(q)$ is a normalized peak-shape function. The summation is over all sets of reflections $\{hkl\}$. Available peak shapes are Gaussian, Lorentzian, modified Lorentzian I and II, pseudo-Voigt, Pearson VII, and a generalized gamma function which in the limits of a continuous parameter becomes a Gaussian or Lorentzian (Förster, Timmann *et al.*, 2005). The scattering intensity as given in equation (2) is normalized such that the integral scattered intensity fulfills Porods law. This approach considers the effect of the particles – *via* the first and second moments of the particle size distribution – and of the lattice – *via* the first and second moments of the distribution of lattice points – on the scattered intensity $I(q)$.

For all structures, only real-space information, such as the form of the object, its size, the relative size distribution, deviations from lattice points and domain sizes, has to be provided by the user. *Scatter* is the only software that uses exact analytical equations for the structure factors of a variety of crystalline or liquid-crystalline lattices and allows fast model calculations and fitting. Since each parameter has its own specific effect on the scattering curves, statistical independence of the fitted parameters is usually given. In particular the parameters and their effects on the scattering curve are unit-cell dimension $\leftrightarrow$ peak position, lattice type $\leftrightarrow$ relative peak positions, domain size $\leftrightarrow$ peak width, displacement $\leftrightarrow$ intensity of higher-order reflections, radius $\leftrightarrow$ position of form factor oscillation, particle shape $\leftrightarrow$ relative positions of oscillations and low-q scaling, and polydispersity $\leftrightarrow$ damping of form factor oscillations.

2.4. Intensity and background

The normalized calculated intensity can be multiplied by a factor I_0 to fit to the measured intensity. A constant (flat) background can be added. It is possible to subtract a measured background file from the data file with a prefactor that is known from the respective measuring time, primary beam intensity and sample absorption and then fixed, or it is possible to adjust the prefactor by fitting.

2.5. Single file and file series fitting

The experimental data are fitted sequentially by a downhill simplex algorithm followed by a Levenberg–Marquardt algorithm. The simplex routine is fast and robust. It allows one to define intervals for the fit parameters to avoid unphysical or meaningless values. After a given number of iterations or if the simplex fit has converged, a fit using the Levenberg–Marquardt algorithm is performed, which gives the fit errors as calculated from the covariance matrix. After fitting, the fitted curve is displayed together with the experimental data and can be saved as an ASCII file.

Scatter provides means to analyze large series of data. During experiments, files are usually stored with consecutive numbering of the file names. If such numbering exists for a given set of files, *Scatter* can automatically read and analyze them by specifying the first and last file to be fitted. If not, a set of files can be stored in a specified folder and loaded from there. More than 10 000 data files can be sequentially loaded, displayed and fitted in a non-interactive mode without requiring user attention. In the automated fitting procedure, the fitted parameters of the previous data set are used as starting parameters for the fit of the subsequent data set. The fitted parameters for a file series are stored as an ASCII spreadsheet together with the fit error. Warnings are given if the covariance matrix indicates mutual interdependence of fit parameters. Fig. 2 shows an example of a fit of a series of 190 scattering curves obtained from a time-resolved measurement at DUBBLE/ESRF.

3. Two-dimensional data primary analysis

Scatter allows the modeling of two-dimensional scattering patterns of oriented and ordered structures and provides tools for optimizing a model and for a direct comparison with the measured scattering pattern. This involves procedures for loading original data, zooming, beam centering, calibration, displaying intensity values numerically and graphically on points, lines and circles, binning, and azimuthal averaging. The loaded image and the intensity scans (lines, circles) can be stored. It is possible to view series of images on stack plots either as intensity scans or as color maps to visualize structural evolutions during the measurements.

3.1. Data input and GUI

Scatter can read common graphic formats that are produced as read outs from detectors at large-scale facility beamlines (ESRF, DESY, ILL, ALS) and laboratory-based equipment. A larger number of formats can be read by *FIT2D* and exported as ASCII spreadsheets (*.spr) that can be imported into *Scatter*. Input data formats include EDF (ESRF/Klora format; *.edf), BSL/OTOKO, raw and T-file output by the ILL D11 and D22 small-angle neutron scattering beamlines, AIDA (*.pcb) used by image-plate detectors, spreadsheets (ASCII) generated by the program *FIT2D* (*.spr), *.img format as used at the Advanced Light Source (ALS, Berkeley Laboratory), *.tif as used by the MarCCD detector, *.tif as used by the Pilatus detector (Dectris), as well as some common formats like bitmap (*.bmp), 8 and 16 bit TIFF, and PNG.

After reading the data file, the scattering pattern is displayed in a separate window with the intensity on a linear or logarithmic scale using a color map that is selected by the user. The minimum and maximum intensity that spans the color map can also be specified. Background files can be loaded and directly subtracted when reading the sample file.

The GUI for the two-dimensional analysis is shown in Fig. 3. It provides all relevant information for viewing and modeling experimental data. It allows the reading of experimental and background data, and loading and saving of parameter files, and provides various plotting options (lin/log, color maps, min/max values, zoom) for the scattered intensity. It guides calibration, averaging and model calculations. It is possible to save experimental data, model calculations, fitted curves, size distributions and density profiles as ASCII data. The graphical data display can be saved as bitmaps and the whole GUI can be printed as a hard copy.

The GUI is organized into different windows and tables. Three large windows contain the experimental data, the model data, and one-dimensional slices of experimental and calculated data. Two small windows display peak positions and a real-space projection of the structure. Three boxes contain the information about the particle, the lattice type and the spatial orientation of the lattice. Additional information, such as a list of peak positions and Porod analysis, can optionally be displayed. Various tools are available for loading, viewing and comparing large series of files.

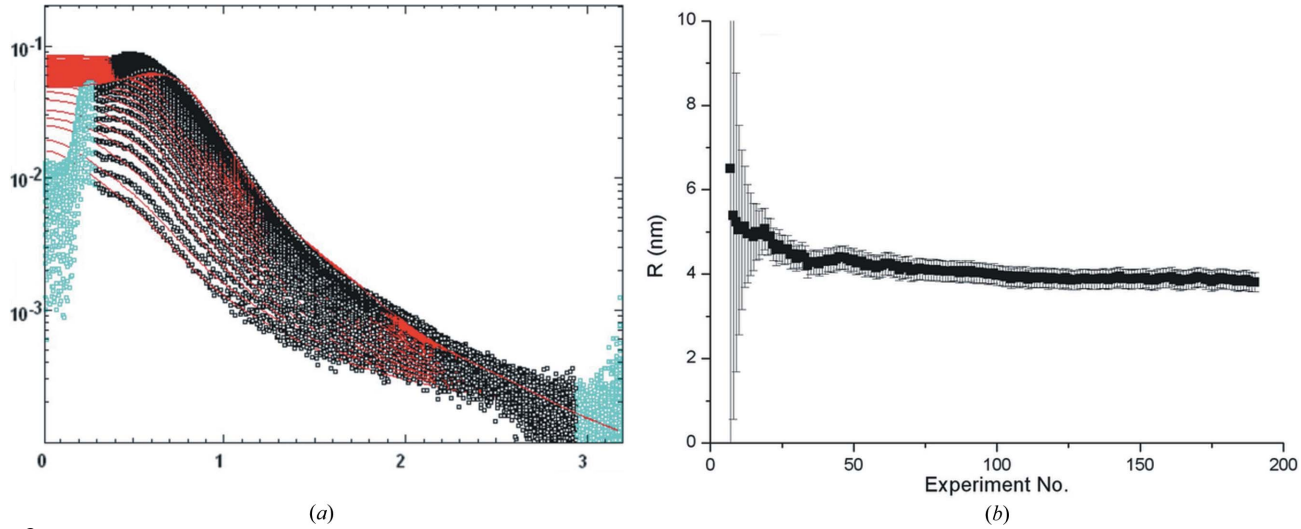

(*a*) (*b*)

Figure 2
Example of 190 scattering curves obtained from a time-resolved synchrotron SAXS experiment that have been sequentially fitted. (*a*) The series of scattering curves together with the fitted curves. (*b*) One of the fit parameters (radius) and its error for each of the measurements. Blue data points were excluded from the fit. The fit for 190 files took 1 min with 100 iterations per file.

3.2. Beam centering and calibration

For the assignment of $\mathbf{q}$ values [$\mathbf{q} = (q_x, q_y, q_z)$] to the pixels of the scattering pattern, the beam position on the detector, the detector pixel size, the sample–detector distance and the wavelength of the beam have to be specified. If these values are contained in the data file header, these are automatically read, displayed and used for the calculations. These values can also be entered manually.

If the beam position is unknown, *Scatter* provides tools to determine the beam position manually, with the use of track bars, by using concentric circles or by calculating the center of gravity. If the sample–detector distance or wavelength is not known, a tool allows its determination with the use of measured calibration samples such as silver behenate or rat tendon (dry or wet). The calibration requires only indication of the positions of the relevant reflections by clicking with the cursor. If all parameters are given, the scattering patterns are displayed together with the correct q scale on the horizontal and vertical detector axes.

3.3. Primary image analysis

The intensity along horizontal and vertical lines or circles on the scattering pattern can be displayed in a separate window. The lines can be tilted with respect to the detector horizontal or vertical, since peak positions or other anisotropic scattering features are often not aligned exactly parallel, but are tilted with respect to the detector horizontal or vertical. It is possible to zoom into the image to analyze smaller features in more detail. Adjacent lines and circles can be binned for better statistics. The intensity along selected lines and circles can be stored as ASCII files.

3.4. Azimuthal averaging

The whole image or a selected sector of the image can be averaged azimuthally to obtain the intensity as a function of the scattering vector $\mathbf{q}$. The obtained scattering curves together with the error in the intensity can be stored as ASCII files and can be loaded and fitted using the one-dimensional module of the software as described above.

3.5. Analysis of data series

Often the user has measured a large series of scattering patterns using the same experimental configuration, *i.e.* the same beam position, sample–detector distance, wavelength and detector settings. Then a horizontal line, a vertical line or a circle can be predefined, a large number of files can be consecutively loaded, and the intensity along this line or circle displayed and/or automatically stored. The files can be loaded according to their consecutive numbering in the file name (up to 10 000 files), or all files are read that have been stored in a common folder. Similarly, a series of files belonging to the same experimental configuration can be azimuthally averaged.

4. Two-dimensional data modeling and fitting

The modeling and in particular fitting of two-dimensional scattering patterns is a challenging task. For example, more than four million data points would have to be fitted for 2k × 2k images of conventional CCD detectors. In principle this can be done, but the calculations would be very time consuming and inefficient. As the number of parameters that describe the majority of features in a scattering pattern are of the order of 10–20, the information contained in different regions of the scattering pattern is highly redundant. It is more efficient to select characteristic features such as peaks, oscillations and geometrical patterns that contain the relevant structural information from the two-dimensional image. By selecting characteristic lines and circles on the image, the analysis can be reduced to a one-dimensional problem. The number of data points can be considerably reduced without loosing relevant information. *Scatter* provides tools to select a set of characteristic lines and circles that can be stored and subsequently fitted to a model. This can be automated to efficiently analyze large sets of two-dimensional data.

The calculations of the scattering patterns $I(\mathbf{q})$ are based on equation (2) where, for the two-dimensional calculations, all three components of the scattering vector $\mathbf{q} = (q_x, q_y, q_z)$ are considered (Förster *et al.*, 2007). The normalized peak-shape functions $L(\mathbf{q})$ are taken either as a product of a radial and azimuthal peak-shape function, or as an anisotropic three-dimensional Gaussian. The peak widths are related to coherence lengths or domain sizes.

4.1. Form factors

Form factors for spheres, cylinders, discs, and unilamellar and multilamellar vesicles are provided. In addition to the one-dimensional case, the length distribution of the cylinders and the distribution of lateral radii of the discs are taken into account. Furthermore, for anisometric particles such as cylinders and discs, the orientational

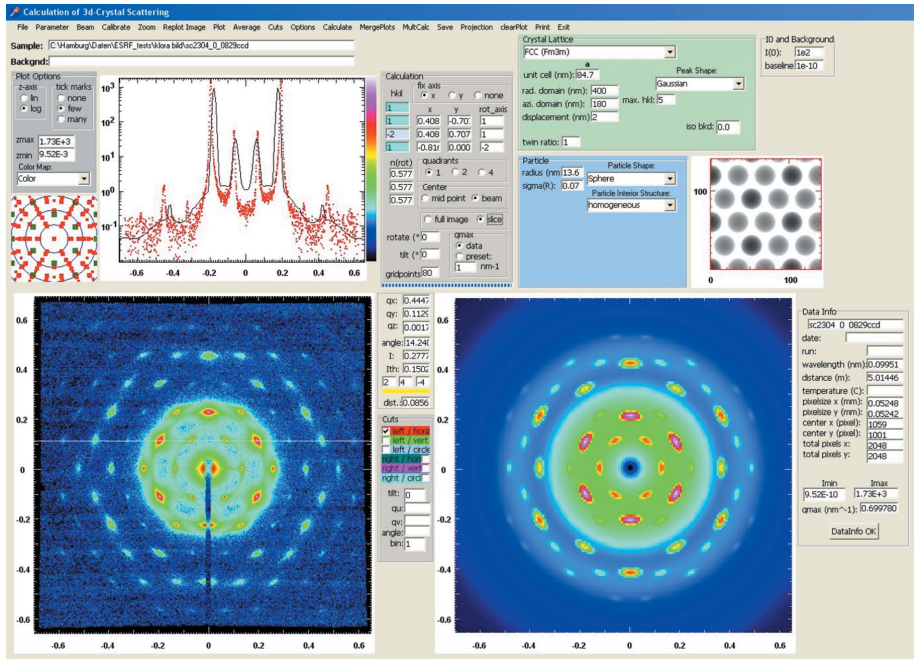

Figure 3
Typical example of the GUI for the two-dimensional analysis, providing information on the particle lattice (green input field), particle structure (blue input field), plot options (gray field) and data. The example shows the analysis of a shear-oriented f.c.c. lyotropic liquid crystal together with the simulation of the scattering pattern and the real-space projection.

distribution with respect to a particular axis can be specified. One can select an isotropic distribution, a perfect orientation, or exponential-, Gaussian-, Onsager-, Maier–Saupe-, cut-off- or Laguerre-type distribution functions. The distribution functions depend on a continuous parameter that is directly related to the mean deviation angle from the director and the orientational order parameter.

4.2. Structure factors

Two-dimensional calculations are possible for the same structure factors as for the one-dimensional case. Many structures, such as f.c.c., b.c.c. and h.c.p., occur in twinned configurations, for which the ratio of the two twins can be specified. Available peak shapes are Gaussian, Lorentzian, modified Lorentzian I and II, pseudo-Voigt, and Pearson VII functions. Peak widths can be different in the radial and azimuthal directions, for each of which a corresponding domain size can be specified. Furthermore, anisotropic Gaussian peaks can be considered, for which the peak widths in each of three orthogonal directions can be specified by giving a corresponding domain size.

4.3. Spatial orientations

The scattering patterns of ordered structures depend on the spatial orientation of the unit cells with respect to the beam. For calculations, the user specifies the direction of the beam and of the horizontal and vertical detector axes (l_x, l_y) in terms of the corresponding *hkl* directions of the unit cell. *Scatter* provides various tools to identify these directions. For a given lattice, it can display the positions of the Debye–Scherrer rings superimposed on the experimental data, with the first Debye–Scherrer ring at the cursor position in the window. If the beam direction is known, the software can make suggestions for or rotate the directions of the detector axes. All three directions are checked for orthogonality. For advanced applications, the *hkl* direction can be rotated around an arbitrary axis to analyze experimental data from rotating single-crystal analysis, where commonly the sample is rotated about the vertical, horizontal or normal axis. Fig. 4 shows model calculations for hexagonally packed cylinders aligned in four different directions. It is also possible to perform multiphase calculations, where scattering patterns for up to three different structures can be stored and their weighted sums calculated and displayed.

4.4. Intensity and background

As for the one-dimensional case, the normalized calculated intensity can be multiplied by a factor I_0 to fit to the measured intensity. A constant (flat) background b can be added. It is possible to subtract a measured background file from the data file. Often there is isotropic background, which can also be considered in the calculation.

4.5. Model calculations of scattering patterns

For a given set of parameters that specifies the form factor, structure factor, lattice orientation, intensity and background, *Scatter* calculates the corresponding scattering pattern in the same q range as the experimental data using the same intensity range and color map, and displays it in an adjacent window to enable quantitative comparison.

Several tools are available for quantitative comparison of experimental and calculated scattering patterns. Moving the cursor on each of the scattering patterns displays the $\mathbf{q}$ value (q_x, q_y, q_z), the azimuthal angle, and the experimental and calculated intensity. Moving the cursor to a peak will display the corresponding *hkl* values and indicate whether it is an allowed or forbidden peak. The user can specify a horizontal, vertical or tilted line or a circle along which the intensities of the experimental and calculated scattering patterns are displayed in a separate window. It is possible to merge sections (quarter or half image) of the calculated pattern into the experimental pattern for quantitative comparison. The images can be saved for publication and presentation. Instead of calculating a whole image, it is also possible to calculate the intensity along selected lines or circles and compare them with the experimental data. This allows a fast optimization of structural parameters to fit the calculated scattering pattern to the experimental scattering pattern.

4.6. Real-space projections and visualization

Similar to transmission electron microscopy, it is often desirable to have a real-space visualization of the corresponding structure. In the case of ordered and oriented samples, a view of the structure in the direction of the beam, in which the scattering pattern was taken, can help to elucidate orientation mechanisms, epitaxial relations or structural transitions. *Scatter* can calculate the projections of the real-space structure using the same parameters and orientation that were used for modeling or obtained from fitting. Furthermore, the calculated projections can be saved as a bitmap.

4.7. Fitting of single and multiple scattering patterns

Since the intensities are calculated from closed analytical equations [equation (3)], it is in principle possible to fit a whole calculated scattering pattern to an experimental scattering pattern. To do this efficiently, lines and circles on the pattern that contain characteristic features such as peaks or form factor oscillations can be selected. A characteristic set of lines and circles can be stored and the calculated

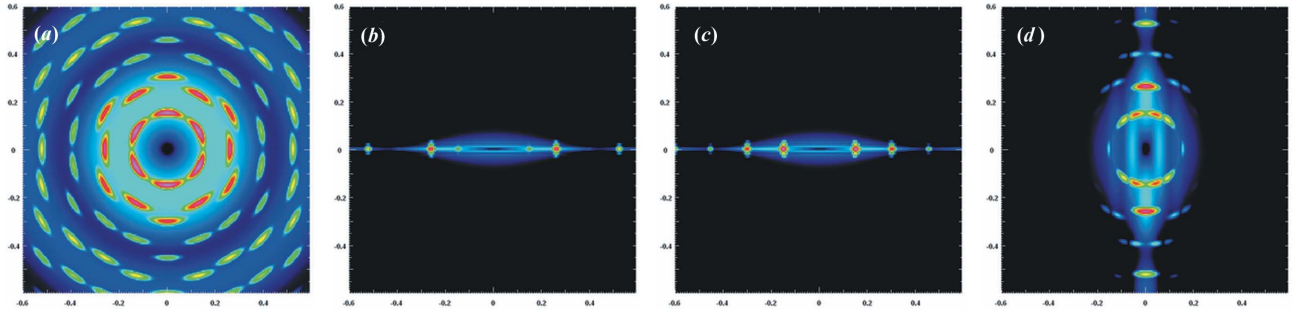

Figure 4
Model calculations for hexagonally packed cylinders. The cylinders are oriented in the (001) direction. Shown are calculated scattering patterns in the (*a*) (001), (*b*) (010), (*c*) (2$\bar{1}$0) and (*d*) (0 1 $\bar{1}$0) directions, *i.e.* slightly off the 001 direction.

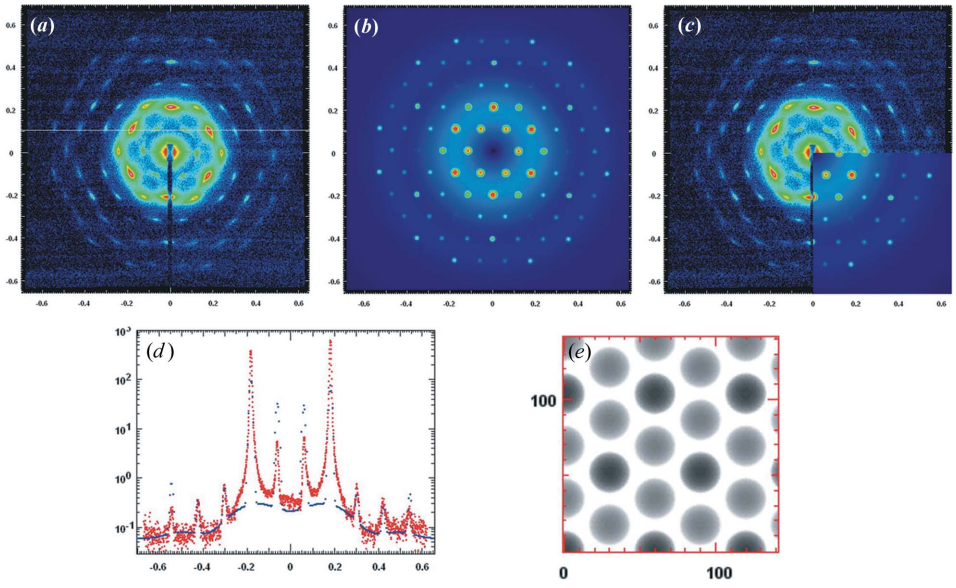

Figure 5
Examples of (*a*) a measured scattering pattern, where the horizontal white line indicates the one-dimensional cut through the pattern, (*b*) the calculated scattering pattern, (*c*) the calculated scattering pattern merged into the measured scattering pattern for quantitative comparison, (*d*) the measured and fitted intensity along the line in image (*a*), and (*e*) a projection of the real-space structure. The measurement is from a shear-oriented f.c.c. lyotropic phase of a block copolymer measured at ESRF.

intensities fitted using the fitting algorithm described above. The fit parameters can then be used to calculate a whole scattering pattern for quantitative comparison (Fig. 5).

The parameters for a one-dimensional fit and each of the additional parameters in a two-dimensional fit have their own specific effect on the scattering pattern so that statistical independence of the fitted parameters is usually given. In particular the additional effects of the parameters in a two-dimensional fit are azimuthal domain size ↔ azimuthal peak width, *hkl* direction ↔ relative peak positions, orientational order parameter ↔ azimuthal intensity distribution of form factor, and polydispersity of cylinder length or disc lateral dimension ↔ damping of form factor oscillations.

The two-dimensional module of *Scatter* has been successfully used to determine the orientational distribution of sheared cylindrical micelles (Förster, Konrad & Lindner, 2005) and to quantitatively analyze the scattering patterns of oriented block copolymer superstructures (Förster *et al.*, 2007). It is currently used for the analysis of lyotropic liquid crystals, nanocomposites, mesoporous structures and quasi-crystals.

4.8. Fitting of series of scattering patterns

If a characteristic set of lines and circles has been selected, it is possible to automatically load a series of scattering patterns, read the intensities along these lines and circles, and store these data in separate files. As described above, this series of files can then be automatically loaded and fitted as in the one-dimensional case. The fit parameters of this series are stored in an ASCII file together with fit errors and possible warnings concerning mutual interdependence of parameters.

4.9. Grazing incidence small-angle scattering

With the advent of more powerful beamlines, grazing incidence X-ray (GISAXS) and neutron scattering (GISANS) techniques are increasingly used. Owing to the interference of scattered and reflected waves, the patterns and their analysis are often more complicated than scattering patterns obtained in transmission geometry. Excellent software packages such as *IsGISAXS* (Lazzari, 2009) exist that take into account interference effects within the distorted-wave Born approximation. For the basic analysis of simple structures such as monolayers of spheres or cylinders on planar surfaces, *Scatter* provides tools for data analysis within the first Born approximation, which neglects interference effects of scattered and reflected waves. For homogeneous monolayers this is often a very good approximation that gives the main structural parameters with good precision. It can serve as a starting point for further refinement using advanced software packages.

For the assignment of **q** values to the pixels of the scattering pattern, the position of the primary beam needs to be specified. For GISAS patterns this is often not possible, because the position of the primary beam is outside the detector area. Therefore the position of the reflected beam is used together with the angle of incidence to assign the **q** values. The position of the reflected beam can be determined with the tools described in §4.2. If both the primary and the reflected beam positions are on the detector, *Scatter* allows one to refine the angle of incidence, which is often not known with sufficient precision.

For a given set of structural parameters, critical angle and surface roughness, *Scatter* calculates the corresponding GISAS pattern in a separate window (Fig. 6). All of the tools for quantitative comparison between experimental and calculated patterns as described in §4.5 can be used. Of relevance is the selection of horizontal lines that are referred to as out-of-plane cuts. These cuts for single or a series of patterns can be stored, modeled and fitted to obtain the basic structural parameters as described in §3.4.

5. Summary, conclusion and outlook

Scatter is the first software that allows the analysis, modeling and fitting of scattering curves and scattering patterns for ordered and

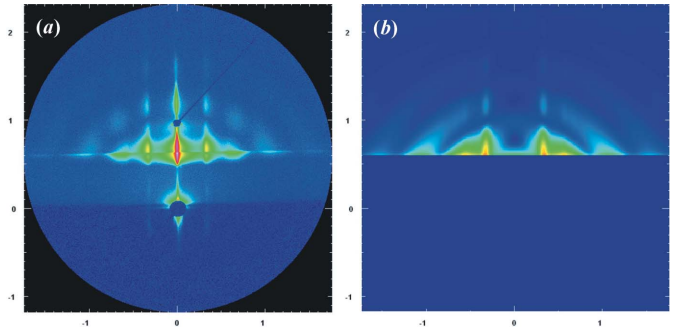

Figure 6
(*a*) Measured and (*b*) calculated GISAXS patterns of a nanoparticle monolayer on an Si wafer as measured at HASYLAB/DESY.

oriented nano- and mesoscale structures. It allows one to fit large series of curves and patterns automatically without requiring user attention. The calculations are based on closed analytical expressions for the scattering intensity. The use of higher transcendental functions provides an efficient evaluation of form factors and structure factors.

Scatter further provides useful tools for data loading, beam centering, calibration, zooming, binning, display and parameter saving. While *Scatter* was developed to support users at the University of Hamburg and DUBBLE/ESRF, it should be generally useful to the small-angle scattering community. It is available free of charge from the distribution web site and is open source for registered users (registration is free of charge). Further improvements that are presently planned are reading of generic data file formats, multiphase fitting, calculation of pair and interfacial distribution functions, contrast calculations, and consideration of smearing effects of primary beam and wavelength distributions.

The authors acknowledge G. Portale (DUBBLE/ESRF) for software testing and making the time-resolved data (Fig. 2) available.

References

Bergmann, A., Fritz, G. & Glatter, O. (2000). *J. Appl. Cryst.* **33**, 1212–1216.
Förster, S. & Burger, C. (1998). *Macromolecules*, **31**, 879–891.
Förster, S., Konrad, M. & Lindner, P. (2005). *Phys. Rev. Lett.* **94**, 017803.
Förster, S., Timmann, A., Konrad, M., Schellbach, C., Meyer, A., Funari, S. S., Mulvaney, P. & Knott, R. (2005). *J. Phys. Chem. B*, **109**, 1347–1360.
Förster, S., Timmann, A., Schellbach, C., Frömsdorf, A., Kornowski, A., Weller, H., Roth, S. V. & Lindner, P. (2007). *Nat. Mater.* **6**, 888–893.
Hammersley, A. P. (1997). *FIT2D: an Introduction and Overview*. Internal Report ESRF97HA02T. ESRF, Grenoble, France.
Hammersley, A. P. (2009). http://www.esrf.eu/computing/scientific/FIT2D/.
Heenan, R. K. (2009). http://www.isis.rl.ac.uk/archive/largescale/LOQ/FISH/instructions.htm.
Heiney, P. A. (2005). *IUCr Commission on Powder Diffraction Newsletter*, No. 32, pp. 9–11.
Heiney. P. A. (2009). http://www.datasqueezesoftware.com/.
Ilavsky, J. (2009). http://usaxs.xor.aps.anl.gov/staff/ilavsky/nika.html.
Ilavsky, J. & Jemian, P. R. (2009). *J. Appl. Cryst.* **42**, 347–353.
Kline, S. R. (2006). *J. Appl. Cryst.* **39**, 895–900.
Kohlbrecher, J. (2009). http://kur.web.psi.ch/sans1/SANSSoft/sasfit.html.
Konarev, P. V., Petoukhov, M. V., Volkov, V. V. & Svergun, D. I. (2006). *J. Appl. Cryst.* **39**, 277–286.
Kotlarchyk, M. & Chen, S.-H. (1983). *J. Chem. Phys.* **79**, 2461–2469.
Koyama, R. (1973). *J. Phys. Soc. Jpn*, **34**, 1029–1028.
Lazzari, R. (2009). http://ln-www.insp.upmc.fr/axe2/Oxydes/IsGISAXS/isgisaxs.htm.
Nielsen, S. S., Toft, K. N., Snakenborg, D., Jeppesen, M. G., Jacobsen, J. K., Vestergaard, B., Kutter, J. P. & Arleth, L. (2009). *J. Appl. Cryst.* **42**, 959–964.
Pedersen, J. S. (1997). *Adv. Colloid Interface Sci.* **70**, 171–210.
Squire, J., Al-Khayat, H., Arnott, S., Crawshaw, J., Denny, R., Diakun, G., Dover, D., Forsyth, T., He, A., Knupp, C., Mant, G., Rajkumar, G., Rodman, M., Shotton, M. & Windle, A. (2003). *Fibre Diffr. Rev.* **11**, 7–19.
Wavemetrics (2008). *Igor Pro*, http://www.wavemetrics.com.